

UNCLASSIFIED

AD NUMBER

ADB007989

LIMITATION CHANGES

TO:

Approved for public release; distribution is unlimited.

FROM:

Distribution authorized to U.S. Gov't. agencies only; Test and Evaluation; MAY 1975. Other requests shall be referred to Air Force Materials Lab., Wright-Patterson AFB, OH 45433.

AUTHORITY

AFWAL ltr 21 Sep 1982

THIS PAGE IS UNCLASSIFIED

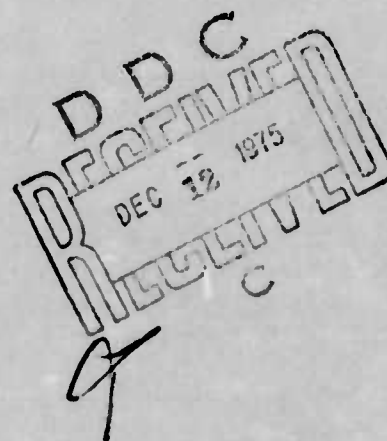
✓ AFML-TR-73-147

Part III

AD B 007 989

GRAPHITE FIBERS FROM PITCH

UNION CARBIDE CORPORATION
CLEVELAND, OHIO



AD No. —
DDC FILE COPY

JULY 1975

TECHNICAL REPORT AFML-TR-73-147, PART III
REPORT FOR PERIOD FEBRUARY 1974 — MARCH 1975

Distribution limited to U.S. Government agencies only; (test and evaluation). May 1975. Other requests for this document must be referred to Air Force Materials Laboratory, Nonmetallic Materials Division, Composite and Fibrous Materials Branch (AFML/MBC), Wright-Patterson AFB, Ohio 45433

AIR FORCE MATERIALS LABORATORY
AIR FORCE WRIGHT AERONAUTICAL LABORATORIES
Air Force Systems Command
Wright-Patterson Air Force Base, Ohio 45433

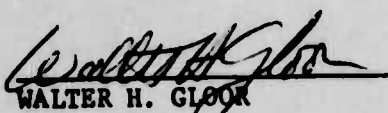
NOTICE

When Government drawings, specifications, or other data are used for any purpose other than in connection with a definitely related Government procurement operation, the United States Government thereby incurs no responsibility nor any obligation whatsoever; and the fact that the government may have formulated, furnished, or in any way supplied the said drawings, specifications, or other data, is not to be regarded by implication or otherwise as in any manner licensing the holder or any other person or corporation, or conveying any rights or permission to manufacture, use, or sell any patented invention that may in any way be related thereto.

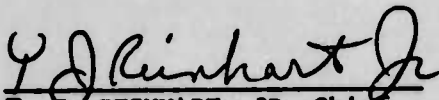
This final report was submitted by Union Carbide Corporation, Cleveland, Ohio under contract F33615-71-C-1538, job order 73200135, with the Air Force Materials Laboratory, Wright-Patterson Air Force Base, Ohio. Walter H. Gloor AFML/MBC was the laboratory project monitor.

This report has been reviewed and cleared for open publication and/or public release by the appropriate Office of Information (OI) in accordance with AFR 17-7 and DODD 5230-9. There is no objection to unlimited distribution of this report to the public at large, or by DDC to the National Technical Information Service (NTIS).

This technical report has been reviewed and is approved for publication.


WALTER H. GLOOR
Project Monitor

FOR THE DIRECTOR


T. J. REINHART, JR. Chief
Composite & Fibrous Materials Branch
Nonmetallic Materials Division

ACCESSION BY	
NTIS	ADONIS SYSTEM
DDC	ADONIS SYSTEM
UNANIMATED	
JUSTIFICATION	
BY	
DISTRIBUTION/AVAILABILITY	
DATE	STAMP
B	

Copies of this report should not be returned unless return is required by security considerations, contractual obligations, or notice on a specific document.

SECURITY CLASSIFICATION OF THIS PAGE (When Data Entered)

REPORT DOCUMENTATION PAGE		READ INSTRUCTIONS BEFORE COMPLETING FORM
1. REPORT NUMBER 18 AFML-TR-73-147-P4-3	2. GOVT ACCESSION NO.	3. RECIPIENT'S CATALOG NUMBER 9 Final
4. TITLE (and Subtitle) 6 GRAPHITE FIBERS FROM PITCH		5. TYPE OF REPORT & PERIOD COVERED Technical Report, Part III Feb 1974 - March 1975
7. AUTHOR(s) 10 R. Didchenko, Principal Investigator		8. CONTRACT OR GRANT NUMBER(s) 15 F33615-71-C-1538
9. PERFORMING ORGANIZATION NAME AND ADDRESS Union Carbide Corporation P. O. Box 6116 Cleveland, Ohio 44101		10. PROGRAM ELEMENT, PROJECT, TASK AREA & WORK UNIT NUMBERS 62101, 7320, 73200135
11. CONTROLLING OFFICE NAME AND ADDRESS DCASR - Cleveland, Federal Office Building 1240 E. 9th Street Cleveland, Ohio 44114		12. REPORT DATE Jul 1975 12 57p.
14. MONITORING AGENCY NAME & ADDRESS (if different from Controlling Office) Air Force Materials Laboratory AFML/ABC Wright-Patterson AFB, Ohio 45433		13. NUMBER OF PAGES 54
15. SECURITY CLASS. (of this report) Unclassified		15a. DECLASSIFICATION/DOWNGRADING SCHEDULE NA
16. DISTRIBUTION STATEMENT (of this Report) 16 AF-7320 17 7320 01 Distribution limited to U. S. Government Agencies only.		
17. DISTRIBUTION STATEMENT (of the abstract entered in Block 20, if different from Report) Same as Report		
18. SUPPLEMENTARY NOTES None		
19. KEY WORDS (Continue on reverse side if necessary and identify by block number) CARBON FIBERS GRAPHITE PITCH		
20. ABSTRACT (Continue on reverse side if necessary and identify by block number) The properties of the multifilament yarn improved over those achieved in the past. Strand tensile strength of up to 2.30 GPa (~350 Kpsi) was measured on fibers with an elastic modulus of 200 GPa (~30 Mpsi). Tests on flat plate composites with epoxy indicated good translation of properties if corrections were made for insufficient fiber loading. The absolute tensile strength of the thin monofilament did not exceed the levels reported in the previous report, but reliable average values in excess of 3.45 GPa (~500 Kpsi) were obtained on filaments with elastic moduli of 300 GPa (45 Mpsi). Attempts to further		

DD FORM 1 JAN 73 1473 EDITION OF 1 NOV 65 IS OBSOLETE

SECURITY CLASSIFICATION OF THIS PAGE (When Data Entered)

402510

* approx.

YB

improve fiber properties by modified thermosetting methods or by processing with tension were not fruitful. Many structural features of the filaments were observed in SEM after etching the fibers in hot air. The monofilament, with random or onion-skin structure, was in most respects similar to "Thornel" 300 fibers. The filaments with radial structure, found in the multifilament yarn, appeared to contain between the oriented ribbons a carbon phase which was considerably more susceptible to oxidation than the ribbons themselves. So far, only gas bubbles and some surface flaws have been identified as major structural defects in Type-P fibers. ↗

PREFACE

The work reported herein was performed under the sponsorship of the Air Force Materials Laboratory, Wright-Patterson Air Force Base, Ohio 45433, Contract No. F33615-71-C-1538, Project No. 7320, Fibrous Materials for Decelerators and Structures, Task No. 732001, Organic and Inorganic Fibers. The technical Direction was provided by Mr. W. H. Gloor, Project Engineer, Composite and Fibrous Materials Branch, Nonmetallic Division, AFML/MBC.

The Contractor is Union Carbide Corporation, Carbon Products Division, Parma Technical Center, P. O. Box 6116, Cleveland, Ohio 44101.

The Principal Investigator is Dr. R. Didchenko. Contributors to the effort are Dr. J. B. Barr, Dr. S. Chwastiak, Dr. I. C. Lewis, Dr. R. T. Lewis, and Dr. L. S. Singer. They are receiving major support from Messrs. J. D. Ruggiero and A. F. Silvaggi, Jr. (Microscopy) and from the Fiber Testing Group under Dr. D. J. Kampe.

This report was submitted on April 30, 1975.

The results of preceding studies are described in Technical Reports AFML-TR-73-174, Parts I and II.

TABLE OF CONTENTS

<u>Section</u>	<u>Page</u>
SECTION I	
INTRODUCTION	1
SECTION II	
SUMMARY	2
SECTION III	
SPINNING OF ULTRAFINE MONOFILAMENT	4
1. Outgassing of Pitch	4
2. Filtration of Pitch	4
3. Filament Uniformity	4
SECTION IV	
PROCESSING AND PROPERTIES OF TYPE-P FIBERS	6
1. Thermosetting of Pitch Fibers	6
2. Single Filament Properties	8
3. Single Filament Strength as a Function of Gauge Length	12
4. Sinclair Loop Test	16
5. Processing Under Tension	24
6. Continuous Processing and Composite Properties	25
SECTION V	
FIBER STRUCTURE	26
1. Formation of the Wedge-like Crack	26
2. Gas Bubbles	26
3. Structural Features of Type-P Fibers Revealed by Oxidative Etching	30
4. Structural Implications of Air-Etching Studies	36
5. Correlation of Fiber Structure with Single Filament Properties	44
REFERENCES	47

LIST OF ILLUSTRATIONS

<u>Figure</u>		<u>Page</u>
1	Cross Sections of Filaments Heated to 600°C After Treatment with 40 Percent HNO ₃ for One Minute	7
2	Cross Sections of Filaments Heated to 600°C After Treatment in Aqua Regia for Five Minutes	7
3	Photomicrographs of Cross-Sections of Carbonized Filaments with Different Amounts of Distortion Because of Insufficient Thermosetting	9
4	Filament Cross-Sections of Moderately Distorted Fibers	13
5	Tensile Strength vs. Logarithm of Gauge Length of Filaments with Different Diameters	17
6	SEM Fractographs of Filaments with Large Holes	18
7	Apparent Stress/Strain Curve for a Monofilament as Calculated from Loop Test	20
8	Scanning Electron Micrograph of a Monofilament Fiber Fractured in Bending	21
9	Scanning Electron Micrographs of a Monofilament Fiber Fractured in Bending	22
10	Scanning Electron Micrograph of a Monofilament Fiber Fractured in Bending	23
11	Bright Field Photomicrographs of Fiber Cross-Sections	27
12	Bright Field Micrograph of Monofilament Cross-Sections with Large Amounts of Voids	29
13	SEM Micrographs of the Fracture Surfaces of 500°C Fibers	31
14	SEM Photomicrograph of Carbonized Fibers Heated in Air at 600°C for 30 minutes	32
15	SEM Photomicrographs of Air-Etched Carbonized Fibers	33
16	SEM Photomicrographs "Thornel" 300 Fibers Etched for 30 Minutes in Air	34
17	SEM Picture of Fractured Type-P Monofilament After Air-Etching at 600°C	35
18	SEM Picture of Fractured Type-P Monofilament After Air-Etching at 600°C	37
19	Scanning Electron Micrograph of a Fiber Processed to 750°C, and Air-Etched at 520°C for 0.5 hour	39
20	Scanning Electron Micrograph of a Fiber from Multifilament Yarn Thermoset by Single Stage Method, Heat-Treated to 750°C, and Air-Etched at 525°C for 0.5 hour	40

LIST OF ILLUSTRATIONS (Cont'd)

<u>Figure</u>		<u>Page</u>
21	Scanning Electron Micrograph of a Fiber from Multifilament Yarn Thermoset by Single Stage Method, Heat-Treated to 1000°C, and Air-Etched at 600°C for 0.5 hour	40
22	Scanning Electron Micrographs of Fibers Processed to 1000°C, and Air-Etched at 600°C for 0.5 hour	41
23	Scanning Electron Micrographs of Monofilament Fibers, Thermoset by Single Stage Method, Heat-Treated to 750°C, and Air-Etched at 525°C for 0.5 hour	42
24	Scanning Electron Micrographs of Monofilament Fibers, Thermoset by the Two Stage Method, Heat-Treated to 1000°C, and Air-Etched for 0.5 hour	43

LIST OF TABLES

<u>Table</u>		<u>Page</u>
I	SINGLE FILAMENT TENSILE STRENGTH TESTS OF DISTORTED FIBERS	10
II	SINGLE FILAMENT TENSILE STRENGTH TESTS OF UNDISTORTED FIBERS	11
III	LONG GAUGE TENSILE STRENGTH AND YOUNG'S MODULUS OF PERFECTLY CIRCULAR FILAMENTS (SAMPLE 14081502)	14
IV	SHORT GAUGE TENSILE STRENGTH DATA FOR SAMPLE 14081502	15
V	COMPARISON OF SINGLE FILAMENT TENSION AND LOOP TESTS FOR MONOFILAMENT FIBERS	19
VI	PROPERTIES OF TYPE-P YARN (1200 FIL.) AND ITS COMPOSITE WITH EPOXY AT NOMINAL FIBER LOADING OF 60 VOLUME-PERCENT	25
VII	FILAMENT PROPERTIES FOR ROUND AND SPLIT FIBERS IN YARN SAMPLE LTF-17E	46

SECTION I

INTRODUCTION

This Technical Report describes the results of the continued effort under Contract No. F33615-71-C-1538. The goal of the Contract is to demonstrate the feasibility of an economic, continuous process for high-performance carbon/graphite fibers from pitch. In view of the results already obtained, the target for the tensile strength of these fibers was raised to ~ 5.5 GPa (800 Kpsi) with an elongation to break of 1.6 percent.

The main emphasis in this report period was on improving the properties of the multifilament yarn and on establishing the ultimate strength levels achievable in ultrathin monofilament. The micro-structure of filaments was extensively studied with the intent to find the strength limiting flaws and to correlate the fiber properties with the various structures found in Type-P fibers.

SECTION II

SUMMARY

The strength of fibers is known to improve with the decreasing filament diameters and/or with the reduced density of flaws. Therefore, spinning of thin, uniform pitch filaments having a minimum of flaws is a necessary prerequisite for achieving the ultimate strength of high performance carbon fibers derived from pitch (Type-P fibers). But even if such perfect mesophase pitch fibers could be obtained, the subsequent carbonization processes could produce numerous structural changes, such as loss of orientation, distortions of filament geometry, formation of porosity, - all of which would have detrimental effects on fiber performance. The ambitious property targets set for the Type-P fibers studied under this Contract, 5.5 GPa (800 Kpsi) for the tensile strength and 345 GPa (50 Mpsi) for the elastic modulus, can be brought within reach only by identifying and eliminating most of the strength limiting structural flaws from the final product. Progress achieved towards this goal during the last Contract period is described in this report.

Continuous monofilament with a diameter of $7.2\mu\text{m}$ and with a standard deviation of only $\pm 0.12\mu\text{m}$ has been spun for extended periods of time. Not every pitch could be spun so well. Filtration through fine stainless steel screens or felts significantly improved the spinnability of most pitches by reducing the content of microscopic solid particles which tend to plug the spinnerette hole. Only partial success was achieved in outgassing the pitch in the spinning pot in order to completely eliminate the occurrence of fine gas bubbles in the monofilament. Such bubbles are still found in some monofilament batches, but they are rarely observed in multifilament yarn.

Insufficient thermosetting of the pitch fibers has been identified as a cause of both low and high properties of the carbonized fiber. In the first case, surface flaws are generated by localized fusion of filaments which have not been completely infusibilized. Filament sticking leads to low strength values both in the strand and in single filament tests. Erroneously high strengths and elastic moduli can be obtained in single filament tests because the circular cross-sections of under-thermoset filaments have become distorted. Under certain test conditions, such distortions can result in erroneously small calculated cross-sections which, in turn, produce too high values of tensile strength and elastic modulus. Nevertheless, after all possible sources of testing errors had been considered, reliable short gauge single filament tensile strengths in excess of 3.5 GPa (~ 500 Kpsi) were repeatedly obtained on filaments with elastic moduli of approximately 300 GPa (45 Mpsi).

Attempts to improve fiber properties by modified thermosetting methods or by processing with tension were not fruitful. The best combination of properties found in strand tests of multifilament yarn consisted of a Young's modulus of 200 GPa (30 Mpsi) and a tensile strength of 2.3 GPa (350 Kpsi). Tests of flat plate fiber-epoxy composites indicated a good translation of properties, but the fiber loading was below that achieved with other carbon fibers. The cause of insufficient fiber loading needs to be established.

A large amount of effort was expended on structural studies aimed at identifying the possible causes of tensile failure in Type-P fibers. Many interesting structural features were revealed by SEM after air etching of fibers at temperatures of 600 - 700°C. The monofilament, which has random to onion-skin structure, responded to a mild oxidative treatment in a manner similar to that of PAN-based carbon fiber, with the core of the filaments eroding faster than the periphery. This behavior implies differences in either graphitic character, crystallite size or porosity between these two regions of the filament. It is still questionable which of these factors is dominant in controlling the rate of etching. Fibers with the radial structure behaved differently. The oxidation was fastest in the regions connecting the oriented lamellae; eventually, the filament disintegrated into ribbon-shaped microfibrils. Air etching of fibers at intermediate processing stages revealed the presence of surface regions more susceptible to oxidation than the rest of the fiber. This phenomenon may simply reflect the well-known catalytic effects of inorganic impurities, but it also may indicate the presence of structural variations which in a less obvious form could exist in the finished fiber. So far, only gas bubbles and surface flaws have been clearly identified as causes of tensile failure. Undoubtedly, other structural flaws of more subtle nature do exist in Type-P fibers and affect their performance. The goal of further studies will be to identify and eliminate these flaws.

SECTION III

SPINNING OF ULTRAFINE MONOFILAMENT

The feasibility of spinning mesophase pitch filaments with diameters below $10\mu\text{m}$ was demonstrated in the preceding contract period. Further effort was aimed at reproducibly spinning filaments with uniform diameter of $\leq 8\mu\text{m}$. Such filaments shrink to approximately 5 - $6\mu\text{m}$ after carbonization, matching the diameters of the thinnest commercial carbon fibers and thus allowing a meaningful comparison of properties.

1. Outgassing of Pitch

Previous experience indicated that gas bubbles dispersed in the pitch in the spinning pot made a truly continuous spinning of monofilament impossible. Several approaches were tried to eliminate this problem. The amount of entrained gases was markedly reduced when the pitch was charged into the pot in form of pellets processed to a density of $1.1 - 1.2 \text{ Mg/m}^3$. Gas bubbles were almost completely eliminated by evacuating the pot while slowly stirring the molten pitch. Unfortunately, this beneficial effect of vacuum did not persist during spinning because the pressurizing gas eventually was beaten into the pitch by the stirrer used to maintain a homogeneous melt and, consequently, the gas bubbles could not be completely eliminated during the monofilament spinning.

2. Filtration of Pitch

Solid particles in the melt are the bane of spinning because they eventually block the spinnerette holes. Therefore, commercial spinning equipment usually is equipped with single or multiple filtering elements, sandpacks, etc. In monofilament spinning, this problem is particularly acute because a single particle can stop the operation. As long as large spinnerette orifices were used, the presence of solid particles was not a serious obstacle to reasonably prolonged spinning. However, when the orifice diameter was reduced, the spinning became practically impossible without previously filtering the pitch.

Two filtering assemblies were used for this purpose. The larger one had a capacity of 200 g. and could be used to filter the entire batch of pitch from the laboratory reactor. The smaller one was just large enough to filter one (30 g.) charge for the monofilament spinning apparatus. The filter media used in the filters were either woven or felt stainless steel screens. These screens were capable of removing particles which could block the finest spinning orifice used, although repeated filtrations were sometimes necessary.

3. Filament Uniformity

Improvements in the spinning art resulted in better uniformity of filament diameters. For instance, in a prolonged spinning test, four rolls of samples containing a total of 16 separate bands of filaments were spun in one hour. The diameters of five filaments were measured in each band which, after removal from the spool, formed a skein with approximately 150 filaments.

The average filament diameters and their errors for each of the four rolls were: $7.5 \pm 0.2\mu\text{m}$, $7.2 \pm 0.2\mu\text{m}$, $7.2 \pm 0.3\mu\text{m}$, and $7.0 \pm 0.2\mu\text{m}$. The average diameter of all of the samples taken together was 7.2 with $\sigma = 0.50$. The filaments spun in this test were quite uniform, especially if one considers the long spinning time and the thermal instabilities inherently present in small equipment.

Further reduction of monofilament diameter is very difficult. Even with the finest spinnerette ever used in these studies and with very well-filtered pitch, the thinnest average diameter of filaments in one of the skeins was $6.8 \pm 0.2\mu\text{m}$ with $\sigma = 0.3$.

Such spinning performance is entirely satisfactory for the evaluation of single filament properties. Frequent presence of gas bubbles, however, puts a limitation on the ultimate strength of fibers, as will be discussed in Section IV 2. of this report. Filaments completely free of voids probably can be obtained only by changing the extrusion mode in the spinning apparatus from pneumatic to mechanical.

SECTION IV

PROCESSING AND PROPERTIES OF TYPE-P FIBERS

1. Thermosetting of Pitch Fibers

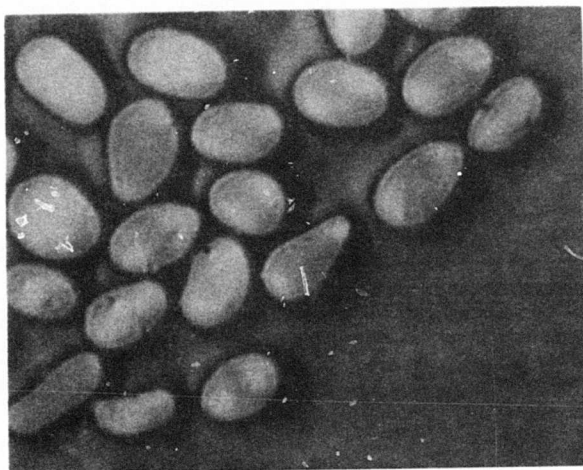
The best properties have been achieved in fibers which had been rendered infusible by first treating the pitch fibers in a proprietary liquid bath and subsequently oxidizing them at elevated temperatures. During the time this work was in progress, other researchers reported many liquid oxidants for processing conventional isotropic pitch fibers.⁽¹⁾ It seemed prudent for us to establish whether some of these agents could be used to advantage with the mesophase pitch fibers. Among numerous liquid oxidants, 40 percent nitric acid and 30 percent hydrogen peroxide were chosen for this study. In addition, aqua regia, which had not been reported, was included because of its known high oxidizing power. The multifilament pitch yarn was treated for 1 to 5 minutes at room temperature in the acid solutions and up to 20 minutes in hydrogen peroxide. Some of the stabilized samples were heated to 600°C in nitrogen and the cross sections examined microscopically to determine the effect of the liquid bath treatment. The remaining fibers were subjected to further oxidation in oxygen followed by carbonization and heat treatment in nitrogen at 1700°C.

The fiber treated in hydrogen peroxide melted when heated to 600°C in nitrogen. The treating solution contained 1 mg/liter of cobaltic chloride in 30 percent hydrogen peroxide. The addition of cobaltic chloride is reported to reduce sticking of the filaments during processing. The hydrogen peroxide solution failed to stabilize the pitch filaments even after treatment times as long as 20 minutes. When the hydrogen peroxide treated fibers were exposed to oxygen at 300°C and then carbonized to 1700°C, the resulting fiber was stiff and brittle. Since such behavior is indicative of inadequate infusibilization, the fibers were not tested further.

The 40 percent nitric acid solution was more reactive towards our pitch fibers. A treatment time of only 1.0 minute partially stabilized the pitch; however, the fibers became distorted when heated to 600°C in nitrogen. The photomicrograph in Figure 1 shows that the surface of the filaments was infusibilized to a depth of approximately 0.5µm, whereas the core of the filaments melted. Cracks may be seen in the skin of some filaments. Even treatment times up to 5.0 minutes in nitric acid and 2.0 minutes in oxygen at 300°C did not completely stabilize the pitch.

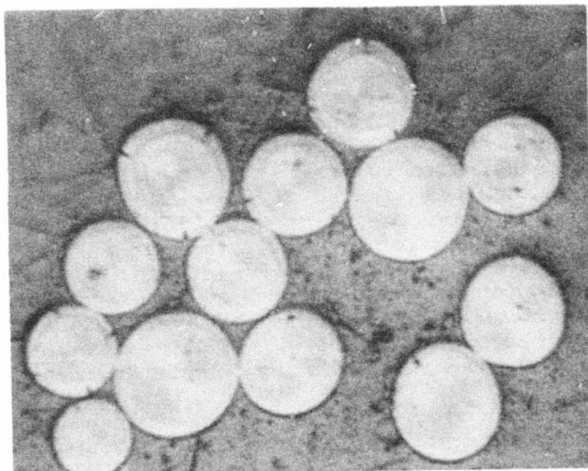
The best average strengths of pitch fibers treated in aqua regia and oxygen was 1.89 GPa (274×10^3 psi), but the handling quality of the fibers was similar to that of fibers prepared with nitric acid. The photomicrograph (Figure 2) of a sample treated for 5.0 minutes in aqua regia and heat-treated to 600°C in nitrogen shows a pronounced skin-core structure. Although most of the filaments have retained their original round shape, the cores have melted, and, in some cases, the pitch has exuded from the center of the filaments. The surface of the filaments was stabilized to depths of 1.0 to 1.5µm.

The same pitch fiber infusibilized in our proprietary liquid bath and heat-treated in oxygen exhibited after carbonization single filament strengths averaging 2.3 GPa (336 Kpsi) and a modulus of 220 GPa (32 Mpsi). Obviously, the aqua regia or nitric acid treatments offer no advantages over the proprietary method which produces multifilament yarn with similar or superior properties.



2000X

Figure 1. Cross Sections of Filaments
Heated to 600°C after Treatment
with 40 Percent HNO_3 for One
Minute.



2000X

Figure 2. Cross Sections of Filaments
Heated to 600°C after Treatment
in Aqua Regia for Five Minutes.

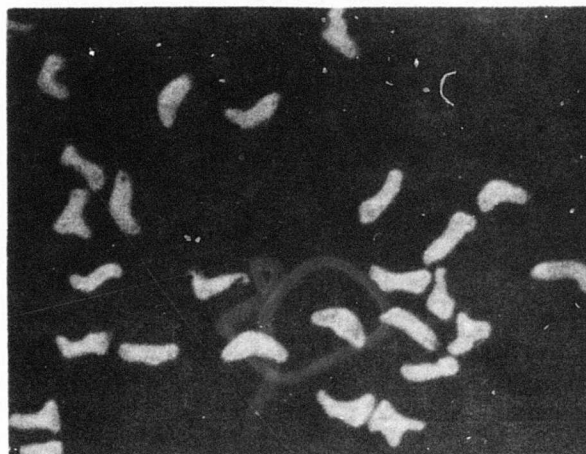
2. Single Filament Properties

Insufficient thermosetting often has deleterious effects on the properties of carbonized yarn, as described previously,⁽²⁾ with both single filament and strand tests reflecting elastic moduli and tensile strengths lower than those of the more severely thermoset fibers. The strand test results are particularly significant because they do not depend on accurate measurements of diameters, since the filament cross-sectional area is derived from the mass of the fibers, their density, and their length. The poor properties of these fibers were ascribed to the filament damage caused by the internal sticking of under-thermoset fibers.

Numerous subsequent single filament measurements of the monofilament properties have shown that erroneously high values can also be obtained as a result of distortion in the circular geometry of filaments which have not been rendered completely infusible. At any given load to break, the apparent tensile strength will be too high when the measured filament diameter is too low. It is easy to see how deceptively low filament diameters can be obtained when ribbon-shaped filaments shown in Figure 3a are treated in the Instron test as if they were cylindrical in shape. Such filaments are often twisted or can become so in the process of mounting them on the Instron tabs. The filament is then scanned under the split-image microscope for the thinnest spot, on the reasonable assumption that the filament will break at that point. In case of a twisted ribbon, the measured diameter may well be the shortest edge of the ribbon which, when treated as if it were the diameter of a circle, would produce a very small apparent area and, consequently, a very high filament strength.

Figure 3b shows the cross sections of a more typical under-thermoset sample taken from a series of fiber samples prepared under different thermosetting conditions from the same batch of pitch filaments with an average diameter of 8.4 μ m. The average diameter measured on 21 filaments of the two least thermoset samples was 5.0 μ m. One of these samples had the highest short gauge tensile strength of the series, 3.2 GPa (470 Kpsi) with a maximum single value of 4.9 GPa (715 Kpsi). Three other samples from the same batch received more severe thermosetting treatment and were completely infusible, as evidenced by the perfectly circular cross-sections of all filaments. The average diameter of 19 filaments from these samples was 5.8 μ m, and the average short gauge strength was 3.4 GPa (390 Kpsi) with a maximum single value of 4.2 GPa (610 Kpsi). The above diameter variations resulted in an area difference of 30 percent which, when used as a correction factor, reduced the highest average tensile strength of the under-thermoset sample to 2.4 GPa (350 Kpsi) - a value very close to the average value of the samples with truly circular filaments.

Less pronounced irregularities in the filament cross-section also can produce very serious errors in the single filament tests. Tables I and II show the computer print-outs of short gauge single filament tests performed on two samples from another series of experiments in which the thermosetting treatments were sufficiently severe so that none of the samples was expected to be distorted. But, again, an unusually high tensile strength of 4.96 GPa (719 Kpsi) was obtained for the least thermoset sample, whereas the tensile strength of 3.20 GPa (460 Kpsi) was typical of all other samples in this series.



1000X

a.



1000X

b.

Figure 3. Photomicrographs of Cross-Sections of Carbonized Filaments with Different Amounts of Distortion Because of Insufficient Thermosetting.

TABLE I

SINGLE FILAMENT TENSILE STRENGTH TESTS OF DISTORTED FIBERS

DATE 02-05-75

SUBMITTED BY R-DIDCHENKO

CHARGE NUMBER

SAMPLE 15013004-8

COMPLIANCE ADJUSTMENT 0.000 MM/GH

MAGNIFICATION/MICROSCOPE CORRECTION FACTOR 0.1818 N/DIV

TO CONVERT GPA TO PSI MULTIPLY GPA NUMBER BY 0.145 X 10⁹

LENGTH (IN.)	BREAKING FORCE (GM.)	COMPLIANCE (0.001 IN./GM.)	C/L (0.001/GM.)	TENS. STRENGTH (GPA)	YOUNGS MOD. (GPA)	AREA (SQ. INCHES)
0.320E 01	0.829E 01	0.000E 00	0.000E 00	0.325E 01	0.000E 00	0.24946E 02
0.320E 01	0.871E 01	0.000E 00	0.000E 00	0.745E 01	0.000E 00	0.11447E 02
0.320E 01	0.710E 01	0.000E 00	0.000E 00	0.670E 01	0.000E 00	0.10383E 02
0.320E 01	0.126E 02	0.000E 00	0.000E 00	0.983E 01	0.000E 00	0.12563E 02
0.320E 01	0.870E 01	0.000E 00	0.000E 00	0.466E 01	0.000E 00	0.17547E 02
0.320E 01	0.500E 01	0.000E 00	0.000E 00	0.327E 01	0.000E 00	0.12952E 02
0.320E 01	0.418E 01	0.000E 00	0.000E 00	0.233E 01	0.000E 00	0.17547E 02
0.320E 01	0.800E 01	0.000E 00	0.000E 00	0.814E 01	0.000E 00	0.18523E 02
0.320E 01	0.589E 01	0.000E 00	0.000E 00	0.277E 01	0.000E 00	0.13732E 02
0.319E 01	0.738E 01	0.000E 00	0.000E 00	0.496E 01	0.000E 00	0.15762E 02

0.46175E 01 STD. DEV. AREA OR 25.6 PERCENT

0.202E-05 STD. DEV. LENGTH OR 0.0 PER CENT

0.274E 01 STD. DEV. BREAKING FORCE OR 57.1 PER CENT

0.000E 00 STD. DEV. COMPLIANCE OR 0.0 PER CENT

0.000E 00 STD. DEV. COMPLIANCE/LENGTH OR 0.0 PER CENT

0.983E 01 MAX. TENSILE STRENGTH (GPA)

0.233E 01 MIN. TENSILE STRENGTH (GPA)

0.252E 01 STD. DEV. TENSILE STRENGTH OR 50.9 PER CENT

0.000E 00 MAX. YOUNGS MODULUS (GPA)

0.000E 00 MIN. YOUNGS MODULUS (GPA)

0.000E 00 STD. DEV. YOUNGS MODULUS OR 0.0 PER CENT

TABLE II
SINGLE FILAMENT TENSILE STRENGTH TESTS OF UNDISTORTED FIBERS

DATE 02-26-75

SUBMITTED BY R-ODICHENKO
CHARGE NUMBER

SAMPLE 15022003-8

COMPLIANCE ADJUSTMENT 0.000 MM/GH

MAGNIFICATION/MICROSCOPE CORRECTION FACTOR 0.1818 M/DIV

TO CONVERT GPA TO PSI MULTIPLY GPA NUMBER BY 0.145 X10⁸6

LENGTH (CM.)	BREAKING FORCE (GM.)	COMPLIANCE (.001 PR/GH.)	C/L (.001/GH.)	TENS. STRENGTH (GPA)	YOUNGS MOD. (GPA)	AREA (SQ. MICROMETERS)
0.320E 01	0.937E 01	0.000E 00	0.000E 00	0.393E 01	0.000E 00	0.23362E 02
0.320E 01	0.110E 02	0.000E 00	0.000E 00	0.403E 01	0.000E 00	0.28268E 02
0.320E 01	0.841E 01	0.000E 00	0.000E 00	0.330E 01	0.000E 00	0.24946E 02
0.320E 01	0.575E 01	0.000E 00	0.000E 00	0.199E 01	0.000E 00	0.28268E 02
0.320E 01	0.100E 02	0.000E 00	0.000E 00	0.419E 01	0.000E 00	0.23362E 02
0.320E 01	0.540E 01	0.000E 00	0.000E 00	0.199E 01	0.000E 00	0.27651E 02
0.320E 01	0.111E 02	0.000E 00	0.000E 00	0.324E 01	0.000E 00	0.33642E 02
0.320E 01	0.100E 02	0.000E 00	0.000E 00	0.291E 01	0.000E 00	0.33642E 02
0.349E 01	0.090E 01	0.000E 00	0.000E 00	0.320E 01	0.000E 00	0.27759E 02

0.41004E 01 STD. DEV. AREA OR 14.7 PERCENT

0.154E-05 STD. DEV. LENGTH OR 0.0 PER CENT
0.231E 01 STD. DEV. BREAKING FORCE OR 25.8 PER CENT
0.600E-00 STD. DEV. COMPLIANCE OR 0.0 PER CENT
0.000E 00 STD. DEV. COMPLIANCE/LENGTH OR 0.0 PER CENT

0.419E 01 MAX. TENSILE STRENGTH (GPA)
0.199E 01 MIN. TENSILE STRENGTH (GPA)
0.004E 00 STD. DEV. TENSILE STRENGTH OR 26.9 PER CENT

0.000E 00 MAX. YOUNGS MODULUS (GPA)
0.000E 00 MIN. YOUNGS MODULUS (GPA)
0.600E 00 STD. DEV. YOUNGS MODULUS OR 0.0 PER CENT

The unusually low cross-sectional area corresponding with a diameter of $4.5\mu\text{m}$ measured on the sample with the high tensile strength, as well as the large standard deviation of the areas and strength values (see Table I), prompted the obtaining of a photomicrograph of filament cross-sections for this sample, which is shown in Figure 4. Indeed, the filaments were not cylindrical, but the distortion appeared far less severe than that observed in Figure 3. However, when the average area of the filament cross-sections in the photomicrograph was measured by means of the Imanco Image Analyzer, a value of $24.6\mu\text{m}^2$ was obtained, which corresponds with a diameter of $5.6\mu\text{m}$. The new cross-sectional area, used to correct the tensile strength of 4.96 GPa, resulted in a value of 3.17 GPa, in very good agreement with the other samples in this series.

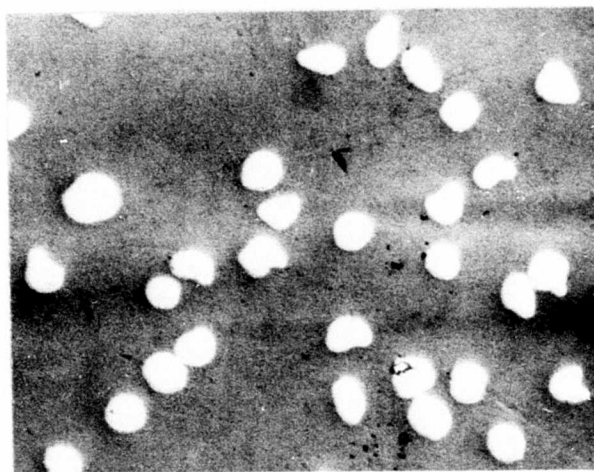
Unusually small filament cross-sections and high standard deviation in the tensile strength measurements must be regarded in the future as warning signals for researchers to exercise great caution before accepting the results. Reliable test results obtained on perfectly circular filaments are shown in Tables III and IV. The standard deviations apparently should not exceed approximately 25 percent for the tensile strength and approximately 20 percent for the area. The closeness of strength values obtained in short and long gauge tensile strengths - 3.54 and 3.32 GPa respectively, (513 and 418 Kpsi) is another indication of uniform properties of these particular fibers.

3. Single Filament Strength as a Function of Gauge Length

The tensile strength of brittle materials is limited by various structural flaws which can act as crack initiators. At any given flaw density, the probability of encountering a flaw in the test specimen is proportional to its volume. In the case of fibers, short and thin filament should be stronger than the thick and long ones. Assuming a reasonably uniform distribution of flaws, one should be able to extrapolate to any desired short gauge length the results obtained at decreasing gauge lengths. For reinforcing fibers, an aspect ratio of approximately 100:1 is considered adequate for the load transfer mechanism to become operative.⁽³⁾ A length of 1 mm satisfies this condition for filaments with diameters below $10\mu\text{m}$.

A series of filament tests was planned to measure the tensile strength of Type-P carbon monofilaments as a function of their thickness and gauge length, to extrapolate the results to 1 mm gauge lengths, to confirm our extrapolated value with actual measurements at 1 mm gauge, and, finally, to compare the outcome of these tests with measurements obtained by the Sinclair loop method, which, in theory, can produce tensile load acting on fiber lengths well below one millimeter. It was hoped that these tests would provide information about the distribution of the strength limiting flaws and give indications of the ultimate strength of Type-P fibers.

Monofilament fibers were spun with raw filaments in size groups with average diameters of approximately 7, 8.5, 10.5, and $12\mu\text{m}$. Each of these groups of filaments was thermoset by using three levels of severity. The infusibilized filaments were processed in the standard manner up to 1700°C . Tensile strengths were determined for 10 filaments of each sample at gauge lengths of 3 mm and 20 mm. The sample with the highest average tensile strength for the two gauge lengths was chosen from each size group to represent the best thermosetting conditions for the given filament diameter.



1000X

Figure 4. Filament Cross-Sections of Moderately Distorted Fibers.

TABLE III

LONG GAUGE TENSILE STRENGTH AND YOUNG'S MODULUS OF
PERFECTLY CIRCULAR FILAMENTS (SAMPLE 14081502)

DATE 09-16-74

SUBMITTED BY R-DIDCHENKO

CHARGE NUMBER

SAMPLE 14081502-1

COMPLIANCE ADJUSTMENT 0.800 MM/GM

MAGNIFICATION/MICROSCOPE CORRECTION FACTOR 0.1818 M/DIV

TO CONVERT GPA TO PSI MULTIPLY GPA NUMBER BY 0.135 X10⁸66

LENGTH (MM.)	BREAKING FORCE (GM.)	COMPLIANCE (.001 MM/GM.),	C/L (.001/GM.)	TENS. STRENGTH (GPA)	YOUNGS MOD. (GPA)	AREA (50. MICROMETERS)
0.192E 02	0.930E 01	0.227E 02	0.114E 01	0.390E 01	0.366E 03	0.23362E 02
0.198E 02	0.128E 02	0.173E 02	0.873E 00	0.318E 01	0.284E 03	0.30482E 02
0.198E 02	0.104E 02	0.212E 02	0.107E 01	0.304E 01	0.272E 03	0.33642E 02
0.198E 02	0.986E 01	0.183E 02	0.924E 00	0.322E 01	0.353E 03	0.30007E 02
0.198E 02	0.118E 02	0.213E 02	0.107E 01	0.325E 01	0.256E 03	0.35537E 02
0.197E 02	0.108E 02	0.201E 02	0.101E 01	0.332E 01	0.306E 03	0.32406E 02
0.61021E-01 STD. DEV. AREA OR 1.65 PERCENT						
0.852E-05 STD. DEV. LENGTH OR 0.0 PER CENT						
0.145E-01 STD. DEV. BREAKING FORCE OR 15.3 PER CENT						
0.226E-01 STD. DEV. COMPLIANCE OR 11.2 PER CENT						
0.114E-00 STD. DEV. COMPLIANCE/LENGTH OR 11.2 PER CENT						
0.390E 01 MAX. TENSILE STRENGTH (GPA)						
0.304E 01 MIN. TENSILE STRENGTH (GPA)						
0.234E 00 STD. DEV. TENSILE STRENGTH OR 10.0 PER CENT						
0.366E 03 MAX. YOUNGS MODULUS (GPA)						
0.256E 03 MIN. YOUNGS MODULUS (GPA)						
0.498E 02 STD. DEV. YOUNGS MODULUS OR 16.2 PER CENT						

TABLE IV

SHORT GAUGE TENSILE STRENGTH DATA FOR SAMPLE 14081502

DATE 09-04-74

SUBMITTED BY R-DIOCHENKO

CHARGE NUMBER

SAMPLE 14081502-2

COMPLIANCE FACTOR 0.000 IN/IN

MAGNIFICATION/MICROSCOPE CORRECTION FACTOR 0.1813 N/DIV

TO CONVERT GPA TO PSI MULTIPLY GPA NUMBER BY 0.145 X10⁸

LENGTH (IN.)	BREAKING FORCE (GM.)	COMPLIANCE (.001 IN/IN)	C/L (.001/GR.)	TENS. STRENGTH (GPA)	YOUNGS MOD. (GPA)	AREA (SQ. IN.)
0.320E 01	0.848E 01	0.000E 00	0.000E 00	0.199E 01	0.000E 00	0.41533E 02
0.320E 01	0.153E 02	0.000E 00	0.000E 00	0.422E 01	0.000E 00	0.35537E 02
0.320E 01	0.149E 02	0.000E 00	0.000E 00	0.396E 01	0.000E 00	0.28452E 02
0.320E 01	0.122E 02	0.000E 00	0.000E 00	0.424E 01	0.000E 00	0.28264E 02
0.320E 01	0.114E 02	0.000E 00	0.000E 00	0.257E 01	0.000E 00	0.43536E 02
0.320E 01	0.124E 02	0.000E 00	0.000E 00	0.263E 01	0.000E 00	0.35790E 02
0.320E 01	0.113E 02	0.000E 00	0.000E 00	0.329E 01	0.000E 00	0.23642E 02
0.320E 01	0.147E 02	0.000E 00	0.000E 00	0.511E 01	0.000E 00	0.28268E 02
0.320E 01	0.131E 02	0.000E 00	0.000E 00	0.363E 01	0.000E 00	0.33642E 02
0.319E 01	0.127E 02	0.000E 00	0.000E 00	0.354E 01	0.000E 00	0.36644E 02

0.63644E 01 STD. DEV. AREA OR 17.3 PERCENT

0.202E-05 STD. DEV. LENGTH OR 0.0 PER CENT

0.222E-01 STD. DEV. BREAKING FORCE OR 18.3 PER CENT

0.000E 00 STD. DEV. COMPLIANCE OR 0.0 PER CENT

0.400E-00 STD. DEV. COMPLIANCE/LENGTH OR 0.0 PER CENT

0.511E 01 MAX. TENSILE STRENGTH (GPA)

0.144E 01 MIN. TENSILE STRENGTH (GPA)

0.993E 00 STD. DEV. TENSILE STRENGTH OR 28.0 PER CENT

0.000E 00 MAX. YOUNGS MODULUS (GPA)

0.000E 00 MIN. YOUNGS MODULUS (GPA)

0.000E 00 STD. DEV. YOUNGS MODULUS OR 0.0 PER CENT

Tensile strength measurements at 10 mm and 40 mm gauge lengths were then made on these samples. Individual filament data were selected from the test results at each gauge length to reduce the coefficients of variation of the cross-sectional areas to ± 10 percent. The resulting samples contained 5 to 9 filaments with diameters at 5.2 ± 0.5 , 6.0 ± 0.4 , 7.4 ± 0.5 , and 9.8 ± 0.7 micrometers.

The average tensile strengths with their coefficients of variation are plotted in Figure 5 versus the logarithm of the gauge length. Such a plot usually results in a straight line relationship if a single mechanism of failure is dominant. Since the value measured at 3 mm gauge for sample A seemed to depress the trend of the other three results, this measurement was repeated. The result was identical. Similarly, repeating the measurements at 20 mm and 40 mm lengths for samples B and D produced results within the standard deviations of the original tests and served to bolster the confidence in the results. The lines drawn through the test points were obtained by a least square approximation. The highest strength, extrapolated to 1 mm gauge length (3.75 GPa) was obtained for sample B. The validity of the extrapolation was confirmed by direct measurements at 1 mm gauge lengths, which gave a tensile strength of 3.6 GPa (523 Kpsi) as an average value of ten breaks with a standard deviation of only 18 percent. All filaments in this test series had an elastic modulus of 225 GPa (34 Mpsi), with a standard deviation of 12 percent. Processing to 1850°C increased the Young's modulus to 340 GPa (49 Mpsi) without affecting the strength. A clear-cut trend of the strength increasing with the decreasing filament diameter was not established in these experiments, although the two thinnest fiber batches were definitely the strongest.

Some relation to the flaw density can be perhaps established by considering the standard deviations of tensile strength as a function of gauge length, obtained during this extensive series of tests. As mentioned above, the standard deviation for 1 mm gauge was 18 percent ($n = 10$). Other values were 16.6 percent for 3 mm ($n = 25$), 35.2 percent for 10 mm ($n = 27$), 23.2 percent for 20 mm ($n = 26$), and 39.1 percent for 40 mm ($n = 24$). The standard deviation in the area ranged from 5 percent to 10 percent. Obviously, the strength of filaments with lengths ≤ 3 mm was much more uniform than that of longer filaments. The flaws which reduce the average strength of filaments below 3.0 - 3.5 GPa (450 - 500 Kpsi) apparently occur with an average frequency of approximately one per 10 mm.

Subsequent studies of filament structure by SEM showed that the fibers used in these studies had a relatively large number of gas bubbles which must be considered as the most likely cause of failure. Some of the holes were quite large relative to the filament diameter, as may be seen in Figure 6. Obviously, such large flaws affect the tensile failure of thin filaments much more than that of the thicker ones, perhaps explaining why a strong dependence of the tensile strength on the filament diameter was not obtained in this series of tests.

4. Sinclair Loop Test

A simple apparatus for performing the Sinclair^(4, 5) loop test on single filaments was constructed. A single filament was formed into a loop confined in a vertical plane between two glass cover slips and lubricated with either glycerine or silicone oil. The fractured fiber ends, imbedded in the viscous liquids, could be preserved for subsequent examination in the SEM.

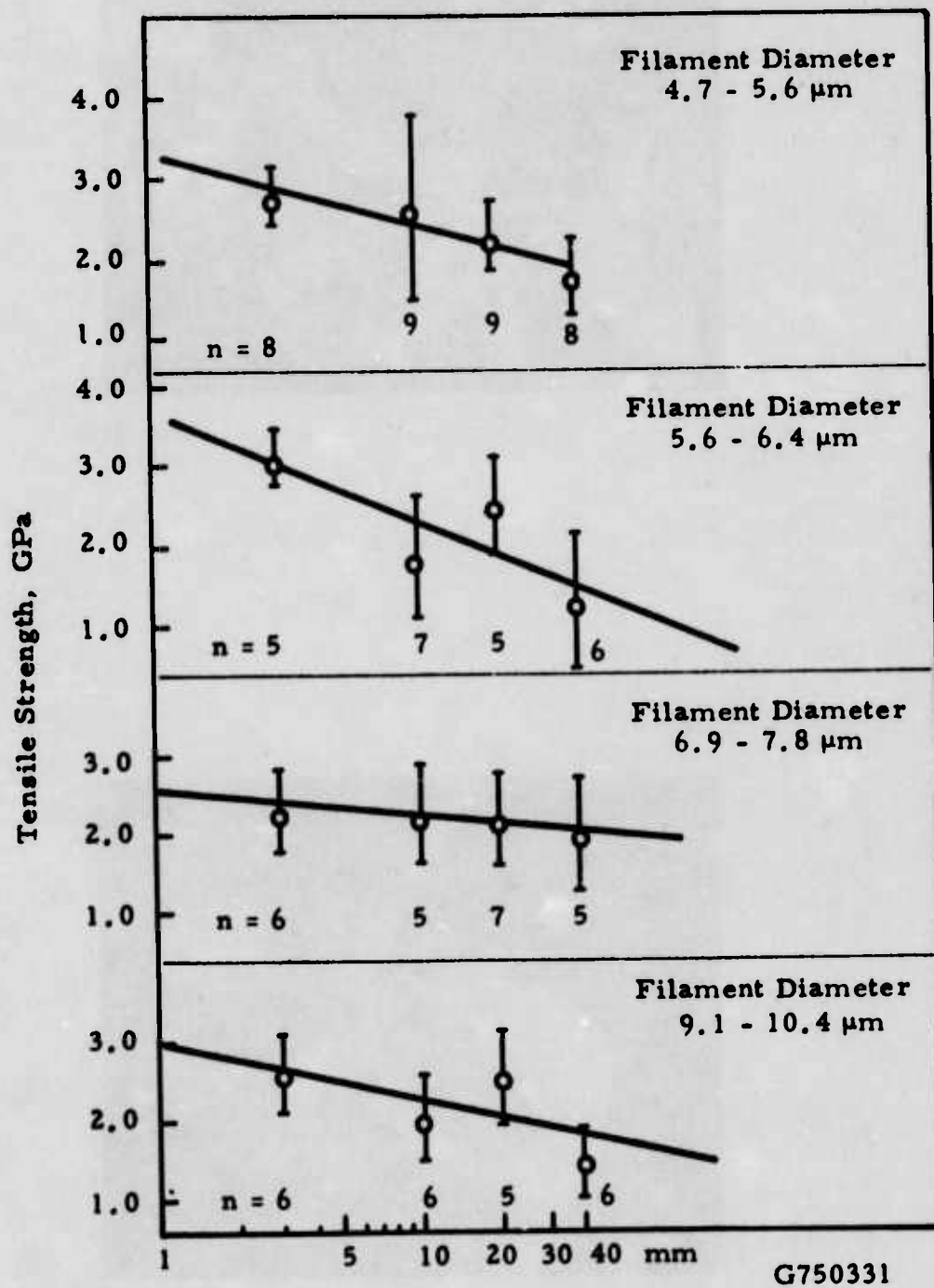
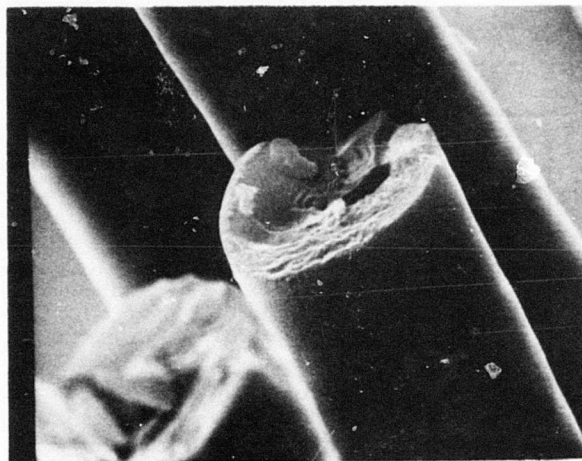
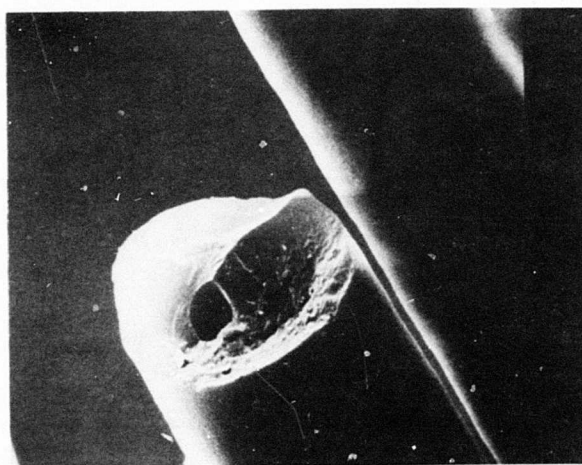


Figure 5. Tensile Strength vs. Logarithm of Gauge Length of Filaments with Different Diameters



4000X

a.



4000X

b.

Figure 6. SEM Fractographs of Filaments with Large Holes

A small hook was fastened to the lower end of the filament, and weights were added until fracture occurred. The corresponding loop diameter at each weight was measured with a traveling microscope. Assuming elastic behavior, Sinclair derived equations for the stress σ , the strain ϵ , and the Young's Modulus E:

$$\sigma = 16wL/\pi d^3; \epsilon = 4d/L; \text{ and } E = 4wL^2/\pi d^4.$$

In these equations, w is the applied weight, L is 3.75D (where D is the loop diameter), and d is the fiber diameter. Ultimate tensile strength was calculated from the data at the highest weight loading prior to fracture. After failure, the diameter of a filament at the point of fracture was measured in a split-image microscope. "Thornel" 300 fibers were used to acquire the necessary fiber handling techniques and to test the apparatus. The Type-P fibers for loop testing were selected from the same monofilament samples which were tested in tension at several gauge lengths as described in Part 2 of this section. These fibers usually broke at loop diameters of ~0.2 mm with ~20 mg on the hook.

After a few loop tests of the Type-P fibers had been made, it became apparent that the stress-strain curves for these fibers were nonlinear. A typical stress-strain curve is shown in Figure 7. The axes are labeled "apparent strain" and "apparent stress" because the values are calculated by using the Sinclair equations which strictly apply only to elastic materials. The curvature of stress-strain curve indicates that considerable deviation from elastic behavior is present. Experimentally, the inelastic behavior was manifested in a flattening of the loop. Table V shows a comparison of the results of single filament tension tests with the calculated values of the loop tests on the same samples. The tensile strength values calculated for the loop test are lower than those for the short gauge tensile test. Calculated modulus values are also lower than the values from single filament testing. The values calculated from the loop test possibly are too low because of spiral distortion of the loop at small loop diameters. When this distortion occurs, the measured loop diameter may be considerably smaller than the true loop diameter. This error could be responsible for the curvature of the stress-strain curves, rather than true inelastic behavior of the fibers in bending.

TABLE V
COMPARISON OF SINGLE FILAMENT TENSION AND
LOOP TESTS FOR MONOFILAMENT FIBERS

Sample	Short Gauge (3 mm) Tensile Strength (GPa)	Loop Test Tensile Strength (GPa)	Fiber * Diameter (μ m)
571-11-71D	2.7	2.5 n = 4	~ 6
571-11-71K	2.2	1.9 n = 2	~ 7
571-11-71T	2.2	1.8 n = 4	~ 9

* At fracture

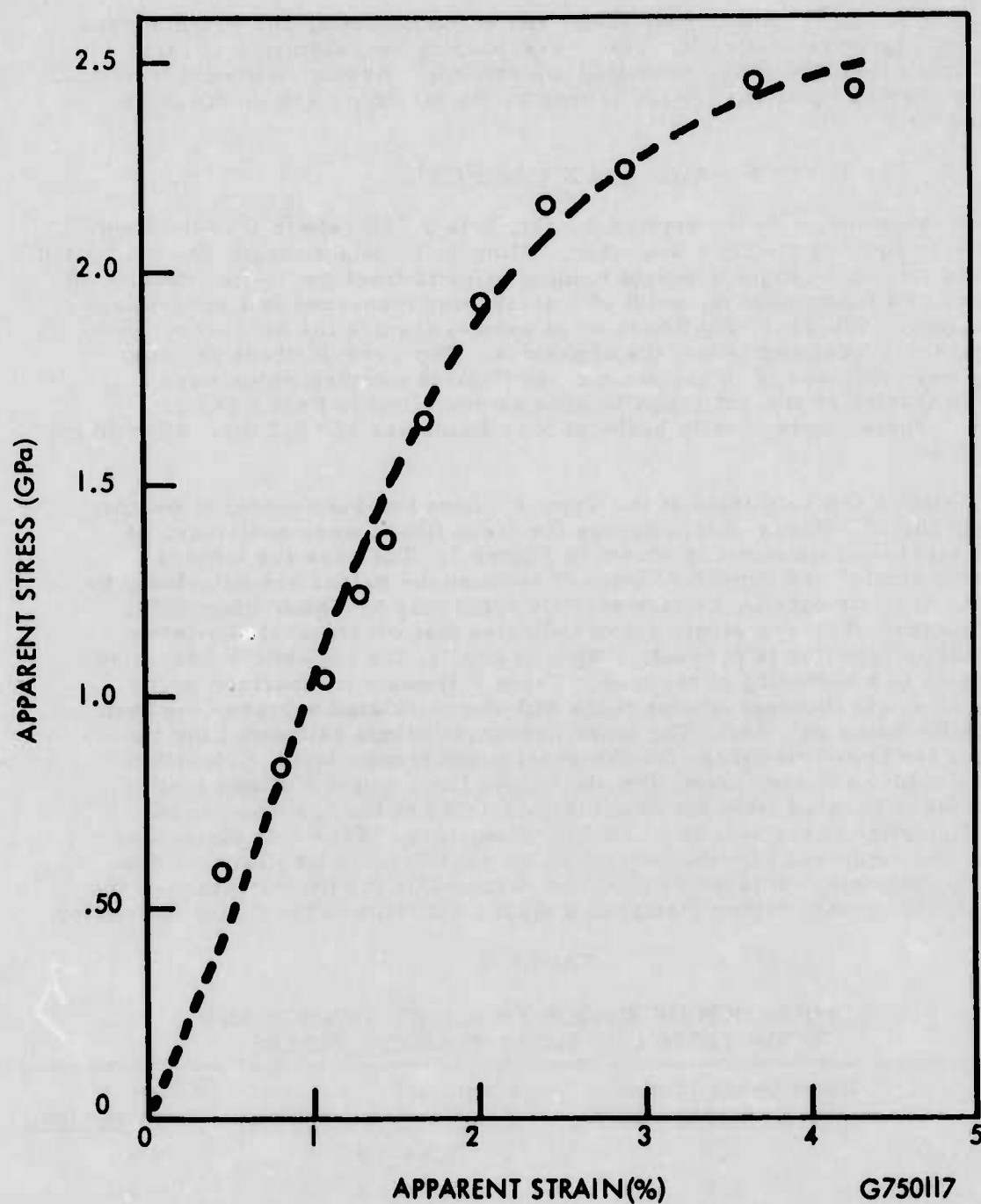
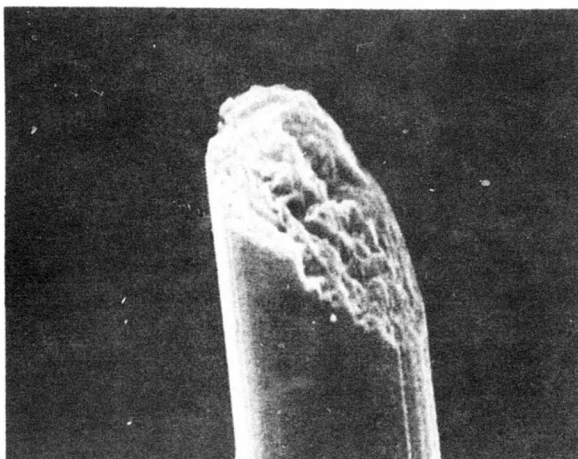


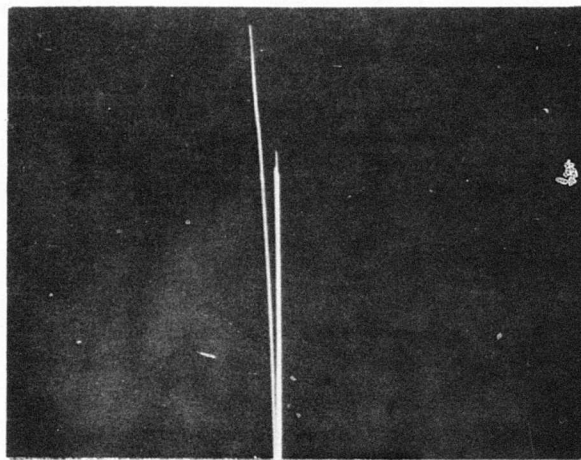
Figure 7. Apparent Stress/Strain Curve for a Monofilament as Calculated from Loop Test

Some of the fractured ends from the loop testing of the pitch fibers were successfully preserved and examined in the SEM. Most of the fractures appeared to be initiated by surface flaws, such as that shown in Figure 8. However, a significant number of the fibers split along the axis, as shown in Figure 9. Another example of a split fiber is shown in Figure 10. In this case, a large portion of the fiber had pulled out during fracture.



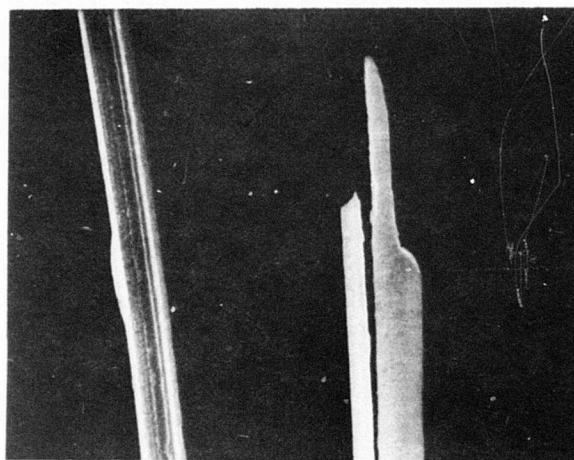
5000X

Figure 8. Scanning Electron Micrograph of a Monofilament Fiber Fractured in Bending.



200X

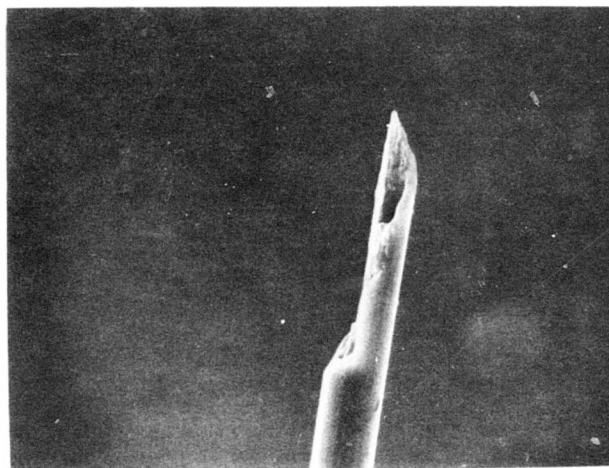
a.



2000X

b.

Figure 9. Scanning Electron Micrographs of a Monofilament Fiber Fractured in Bending at a. 200X, and b. 2000X



5000X

Figure 10. Scanning Electron Micrograph of a Monofilament Fiber Fractured in Bending

5. Processing Under Tension

It is well known that the degree of orientation of many polymer fibers can be enhanced by stretching the fibers at slightly elevated temperatures. Stretching of carbon fibers at very high temperatures ($> 2500^{\circ}\text{C}$) produces a high degree of preferred orientation and also a very significant improvement in elastic moduli. Recently, it has been reported⁽⁶⁾ that external stress applied to conventional pitch fibers during processing to 1000°C had resulted in increases of 20 percent in the elastic modulus and increases of 40 percent in the tensile strength of the carbonized fiber. Because of the poor strength of these pitch fibers, the applied tension was only approximately 7 mg/filament denier.

Mesophase pitch fibers seem to lose only very little of their preferred orientation in the carbonization process,⁽⁷⁾ but some degradation of this property has been detected in X-ray diffraction.⁽⁷⁾ Consequently, it seemed desirable to establish whether processing under tension would also improve the properties of Type-P fibers. Before tensioning experiments were performed, the shrinkage of the yarn was determined at four processing stages. No changes in length occurred in the liquid thermosetting bath. Further gaseous oxidation at elevated temperatures resulted in a shrinkage of 4.1 percent. The total shrinkage after carbonization at 1000°C was 9.5 percent. Surprisingly, after it was passed through a furnace kept at 1650°C , the same yarn showed a total shrinkage of only 8.6 percent. Some stretching of the yarn apparently occurred at this stage, although very little tension was used to pass the yarn through the furnace. Very likely, this change is an apparent elongation which reflects a straightening of the somewhat wavy thermoset yarn.

In the stretching experiments, the thermoset yarn was heated in the temperature range 450°C to 920°C in a vertical furnace while being subjected to an increasing stress by means of suspended weights. In general, the yarn would support loads of approximately 60 mg per filament denier, almost ten times larger than those mentioned in Reference 6. Occasionally, loads of 300 mg per filament denier could be applied, but in no instance was the shrinkage of the fibers kept under load during heat-treatment any different from that of the unstressed fiber. It is not surprising, therefore, that the carbon fiber tensile strength and Young's modulus were not affected by the tension. Correspondingly, there appeared to be no effect at these stress levels on the crystallite alignment with respect to the fiber axis or on the stack heights L_c as determined from X-ray analysis of the carbonized fiber.

To ensure, however, that some conditions under which stretching might occur were not missed in the stationary experiments, Type-P fibers were processed through 1700°C with loads up to 84 mg/denier. Loads were applied during infusibilization in oxygen, at all carbonization stages, and in the final heat-treatment at 1700°C . Weights were hung on the fiber in increasing amounts until the yarn reached the breaking point. Processing was carried out with the highest weight the fiber would support.

Since the fiber would not support a load as low as 6 mg/denier during infusibilization in oxygen, it could not be processed through this stage under tension. The tension which could be applied to the fiber during processing at 1700°C was determined by the strength of the 1000°C heat-treated material. Consequently, the loads through the 700° to 1000°C step and the 1700°C heat-treatment were nearly the same. The strand tensile strength (1.65 to 1.83 GPa)

and the Young's Modulus (214 - 269 GPa) measured on these fibers were identical, within experimental errors, to those obtained on the same batches of fibers processed without tension.

6. Continuous Processing and Composite Properties

Multifilament yarn samples (3/240) in approximately 100 meter lengths have been repeatedly processed in the laboratory continuous line with the final heat treatment at 1650° - 1700°C. Carbon yarn with strand tensile strength exceeding 1.75 GPa (250 Kpsi) was obtained routinely. On several occasions, the product had average strand strength of 2.0 GPa (~ 300 Kpsi) and a modulus of 200 GPa (~ 30 Mpsi), with high values of the strength reaching 2.4 GPa (350 Kpsi). It would have been very time-consuming and costly to accumulate in laboratory-scale equipment sufficient amounts of such yarn for meaningful composite tests.

Almost simultaneously, much larger quantities of 1200 filament Type-P yarn with only slightly inferior properties were being produced and tested in composites within the Fiber Technology programs funded by the Union Carbide Corporation. Table VI shows the properties of these fibers and the properties of a flat plate made with these fibers and epoxy resin. For purposes of comparison with other carbon fiber composites, the results were normalized to 60 volume percent of fibers, since it was difficult to obtain such high fiber loading with these experimental fibers, probably because the yarn was not properly collimated. Nevertheless, a very good balance of the tensile and compressive behavior was achieved. The tensile strength was actually higher than expected from the fiber strand properties. The composite properties seem to better reflect the single filament properties, which commonly are approximately 20 percent higher than the strand test results.

TABLE VI

PROPERTIES OF TYPE-P YARN (1200 FIL.) AND ITS COMPOSITE
WITH EPOXY AT NOMINAL FIBER LOADING OF 60 VOLUME-PERCENT

<u>Fiber (Strand)</u>	<u>GPa</u>	<u>Kpsi</u>
Tensile Strength	1.48	213
Young's Modulus	190	27.5×10^3
<u>Composite (Flat Plate)</u>		
Tensile Strength	1.06	153
Compressive Strength	1.01	147
Flexural Strength	1.03	149
Young's Modulus	99.3	14.4×10^3

SECTION V

FIBER STRUCTURE

The various microscopic methods used to study the structure of pitch and carbon filaments have been described in the previous Technical Report.⁽⁸⁾ Three types of transverse structures in the as-spun fibers (radial, onion skin, and random) have been identified by polarized light microscopy. The "missing wedge" structure has been observed by SEM in multifilament yarn, and the presence of this flaw has been related to the radial structure of the as-spun fiber. Results of continued structural studies by optical microscopy and SEM will be discussed in this section.

1. Formation of the Wedge-like Crack

Formerly, the multifilament fiber had exclusively a pronounced radial structure which resulted in nearly all carbonized filaments having a "missing wedge"; more recently, the filaments in the yarn have often shown a mixture of structures, radial and random. On occasion, yarn with purely random filaments, completely free of cracks, has also been produced.

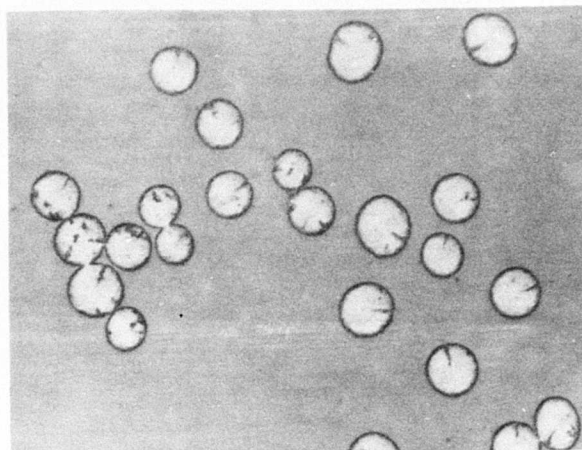
The crack in the filaments with radial structure is very narrow and often invisible in the as-spun state, but widens to a considerable extent during carbonization. A series of samples from different stages of processing was examined by optical microscopy to determine the extent of crack opening at each stage.

Figure 11a shows a photomicrograph of the as-spun fibers used for this investigation. The cracks are initially very narrow and remain quite narrow after thermosetting and carbonization at 450°C (Figure 11b). Even after heating to 700°C, most cracks are not wider than approximately 15 degrees of angle (Figure 11c). However, after the fibers were carbonized at 1000°C, the cracks opened to an angle of approximately 45 degrees in most of the fibers (Figure 11d).

The densities of the fibers at these stages of processing were 1.35 Mg/m³ at 450°C, 1.37 Mg/m³ at 700°C, and 1.72 Mg/m³ at 1000°C. Thus, cracks open to an appreciable extent in the temperature range where shrinkage begins to occur. The radial structure of the fibers, which would be expected to produce anisotropic shrinkage, tends to enhance this crack opening.

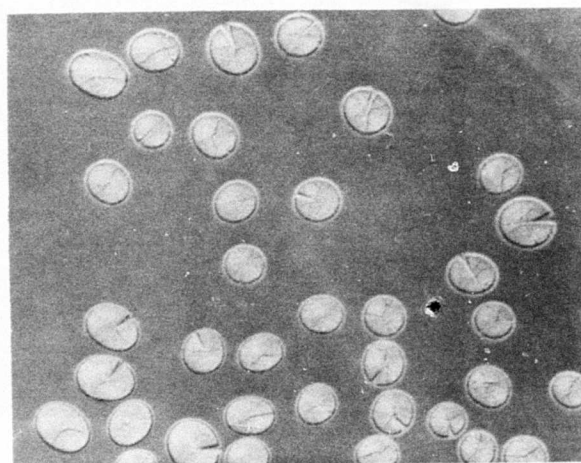
2. Gas Bubbles

Apart from the crack and surface flaws, gas bubbles are the only other gross flaws that have been so far identified in Type-P fibers. The gas bubbles are found only rarely in the multifilament yarn, but they are more common in the monofilament. Figure 12 shows a bright field photomicrograph of an as-spun monofilament bundle with an unusually high concentration of voids.



500X

a.



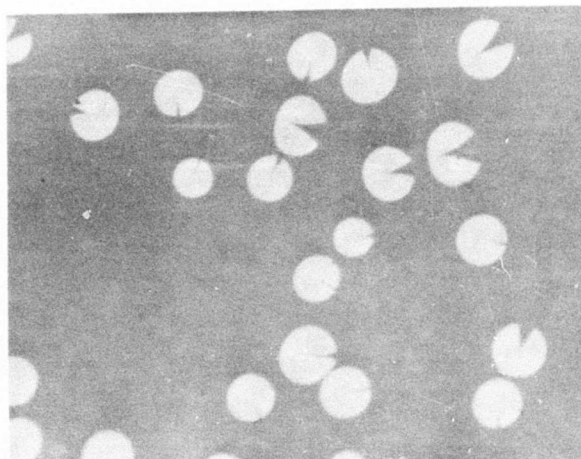
500X

b.

Figure 11. Bright Field Photomicrographs of Fiber Cross Sections

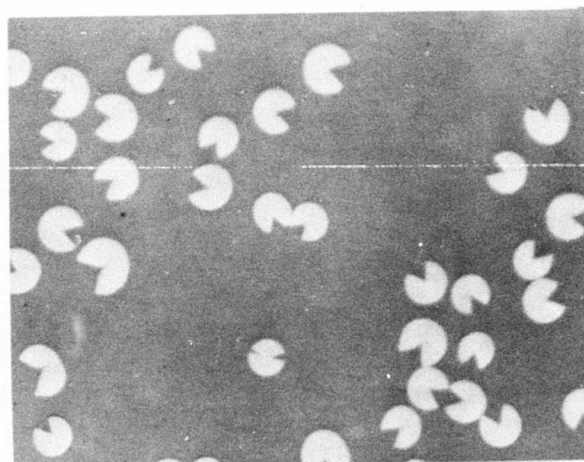
a. As-spun fibers.

b. Fibers thermoset and carbonized to 450°C. (Some additional fine cracks have been produced by polishing)



500X

c.



500X

d.

Figure 11. (Continued)

- c. Fibers carbonized to 700°C.
- d. Fibers carbonized to 1000°C.

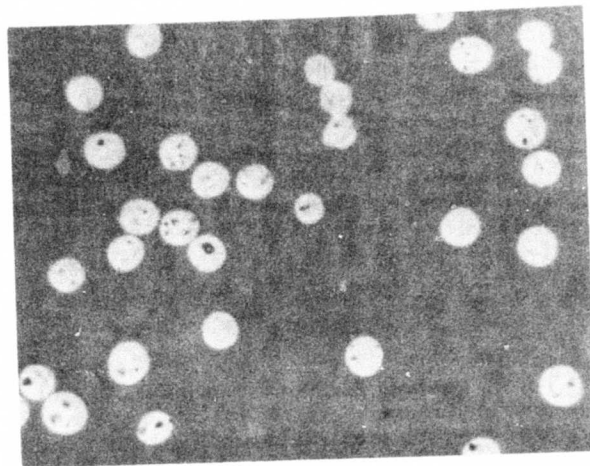


Figure 12. Bright Field Micrograph of Monofilament
Cross-Sections with Large Amounts of Voids

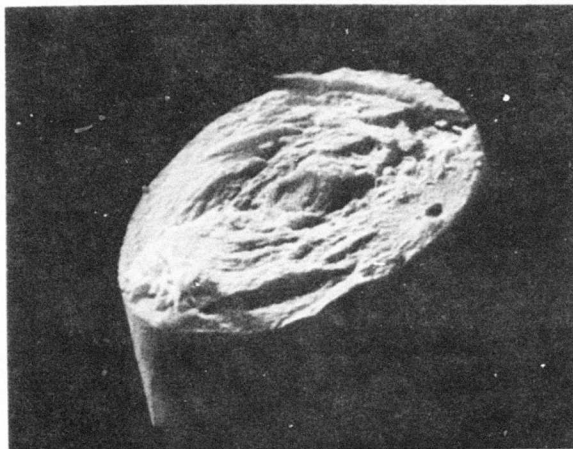
When fracture surfaces of the 500°C HT fibers were examined by SEM, many fractures were found to be initiated at these pores. Figure 13a shows a fracture surface where the failure appears to have started at a small pore close to the edge of the fibers. Figure 13b shows a fracture at a large pore located more centrally. The appearance of the fracture surfaces is consistent with the onion skin structure of these fibers determined by polarized light microscopy.

3. Structural Features of Type-P Fibers Revealed by Oxidative Etching

Etching with oxygen plasma has been used⁽⁹⁾ in SEM studies of the structure of PAN-based carbon fibers. Simple controlled oxidation in hot air prior to observation in SEM has been used in the present study to reveal very effectively several structural features previously only deduced from fractography and polarized light microscopy. Bundles of continuously processed fibers heat-treated to 1650°C were cut with a sharp scalpel blade. Etched samples were prepared by placing the cut bundles into a boat in a tube furnace and heating for 30 minutes at temperatures of 550° to 750°C in a slow flow of air. After this etching procedure, the cut ends of the fibers were examined in the SEM. The effectiveness of the etching strongly depends on the temperature. An SEM photomicrograph of a fiber etched in the air at 600°C is shown in Figure 14. This surface is similar to the fracture surface for unetched fibers; detectable etching effects are not apparent. Figure 15a shows the end of a fiber etched at 650°C in air. The effects of the air-etching are becoming visible, clearly exposing the radial structure and partially revealing the domain or "fibril" structure of the filament. Figure 15b clearly shows the elongated domains, parallel to the fiber axis, obtained after etching the filament at 700°C. These elongated domains correspond with the domains seen by polarized light microscopy of longitudinal sections.

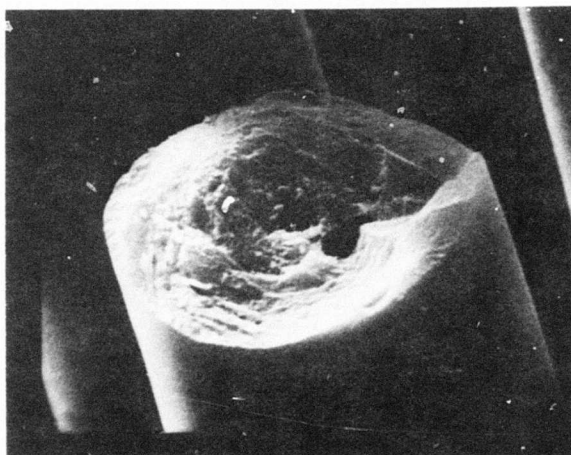
So that structural differences between PAN and pitch-based fibers might be revealed, the hot air etching method was also applied to a sample of "Thornel" 300 carbon fibers derived from PAN. The latter were considerably less resistant to oxidation than the pitch-derived fibers. Etching of "Thornel" 300 fibers for 30 minutes at 500°C resulted in approximately the same level of oxidation as that produced in Type-P fibers after 30 minutes in air at 600°C. The structure of the fractured "Thornel" 300 fibers after etching also was considerably different from that of the Type-P fibers. A typical SEM photomicrograph of "Thornel" 300 fiber etched at 500°C is shown in Figure 16. The center of the fiber has been etched more than the edge, leading to a concave surface. A typical SEM photomicrograph for a more severely etched fiber (525°C) is shown in Figure 16b. Even though the fiber diameter has been reduced by the more extensive hot air etching, the concave appearance of the fiber end is still readily apparent.

The etching behavior of the Type-P monofilament is different from that of the multifilament yarn with its pronounced filament radial structure and, in some respects, it is similar to PAN-based carbon fibers. Figure 17 shows a representative SEM picture of a monofilament after it was cut with a scalpel blade and given a mild air-etching at 600°C for 30 minutes. Apparently, there was a skin-core structure in the fiber and the core was oxidized preferentially by the hot air. The skin-core structure results from the two-stage infusibilization method.



3500X

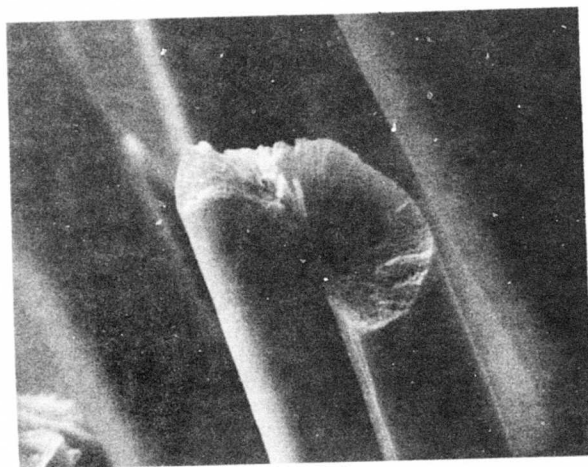
a.



3000X

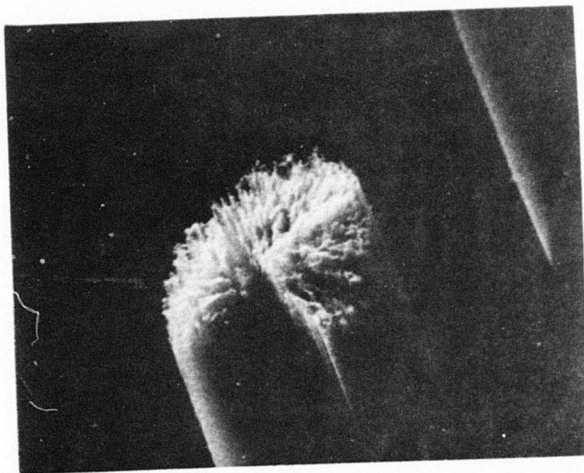
b.

Figure 13. SEM Micrographs of the Fracture Surfaces of 500°C Fibers



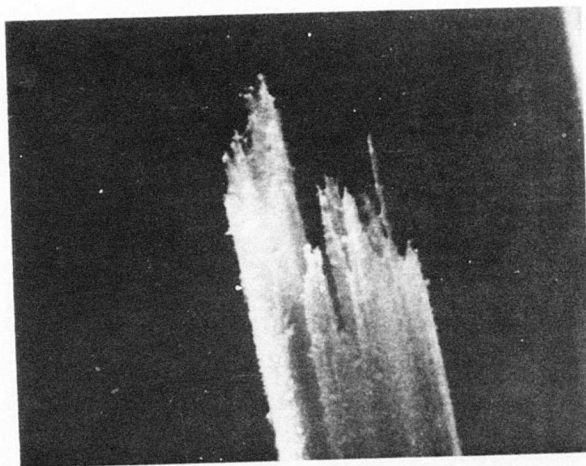
3000X

Figure 14. SEM Photomicrograph of Carbonized Fibers
Heated in Air at 600°C for 30 Minutes



3000X

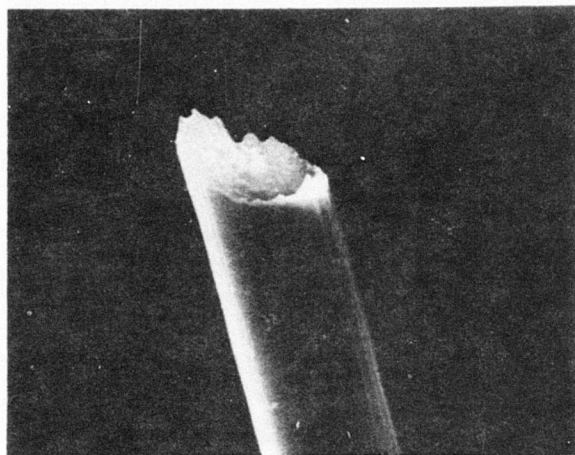
a. 650°C



3000X

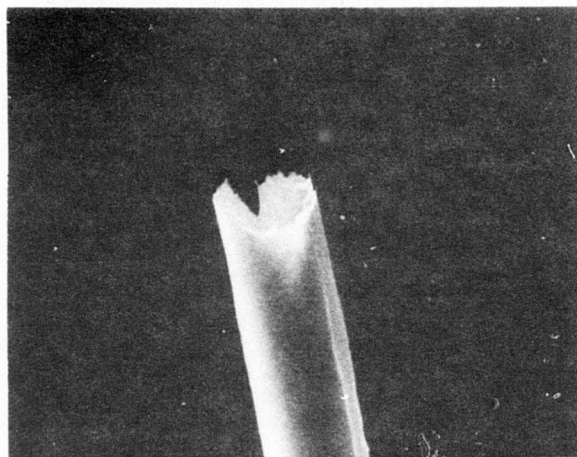
b. 700°C

Figure 15. SEM Photomicrographs of Air-Etched Carbonized Fibers



3000X

a.



3000X

b.

Figure 16. SEM Photomicrographs "Thorne!" 300 Fibers Etched at
a. 500°C and b. 525°C for 30 Minutes in Air



3000X

Figure 17. SEM Picture of Fractured Type-P Monofilament
After Air-Etching at 600°C

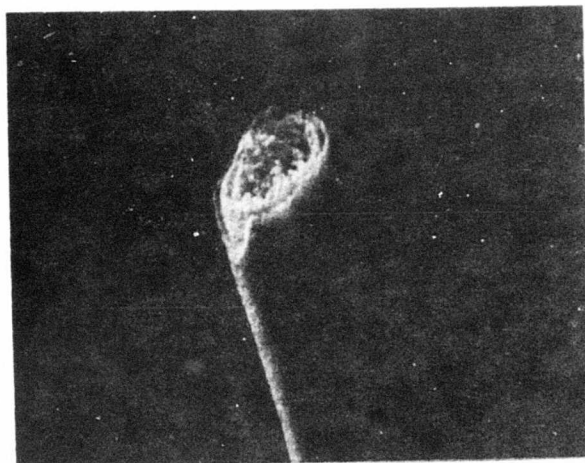
The presence of a very thin skin is also apparent in a similarly etched monofilament from another sample (Figure 18). Insufficient thermosetting of this sample resulted in oval rather than circular filament cross-sections. Air-etching has considerably enhanced the skin-core effect. In addition, a piece of the skin is missing from one edge of the fiber. Presumably, this piece flaked off during the cutting of the fiber with the scalpel. Such behavior indicates a relatively weak bond between the skin and core in the fiber.

4. Structural Implications of Air-Etching Studies

The air-etching of PAN-based carbon fibers shows that the oxidation resistance varies considerably from the surface to the core of the filaments. This behavior reflects the well-established⁽¹⁰⁾ decrease in crystallite size and orientation extending from the surface to the periphery of the filaments. The different response of Type-P fibers to air-etching indicates that these fibers must have some different structural features which affect the oxidation rate. In general, the skin, which is derived from pitch that has been oxidized more severely than the material in the core of the fiber, should be less crystalline, less dense, and, therefore, more susceptible to oxidation. This condition appears to prevail in radial filaments from the multifilament yarn. The radial-lamellar appearance of these filaments after air-etching is perhaps enhanced by the presence of a less-ordered, more oxidizable carbon phase between the lamellae.

It was mentioned above that the Type-P monofilament resembles more the "Thornel" 300 fibers in its etching behavior (i.e., the core is more susceptible to oxidation than the periphery of the fibers). Two explanations are possible: the first is that, because of the onion-skin orientation, the surface of the fibers is similar to the c-plane of graphite which is more oxidation resistant than the a-plane; the second explanation would put the blame for the more rapid oxidation of the core on its having a more highly developed micro-porosity than the skin. Much more refined structural studies would be needed to resolve these ambiguities.

Air etching of P-type fibers at several intermediate processing stages provided some additional insight into their structure. Fibers heat-treated only to 750°C deserved closer scrutiny because surface area measurements of fibers at different processing stages had shown that the surface area of fibers thermoset and heat-treated to this temperature was much higher than that of the original thermoset fibers or the carbonized (1650°C) fibers. Fibers processed to 1000°C were included because, at this temperature, the chemical carbonization processes are essentially completed. In view of the previously described skin-core structures, air etching studies were made on fibers thermoset by both the single stage and the two-stage procedures. It was hoped that any effect of different thermosetting methods on fiber structure would be more likely revealed at lower heat-treatment temperatures rather than at more advanced stages of carbonization.

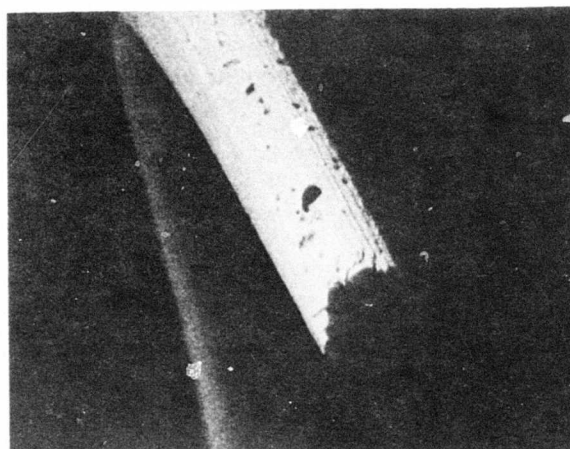


3000X

Figure 18. SEM Picture of Fractured Type-P
Monofilament after Air-Etching at 600°C

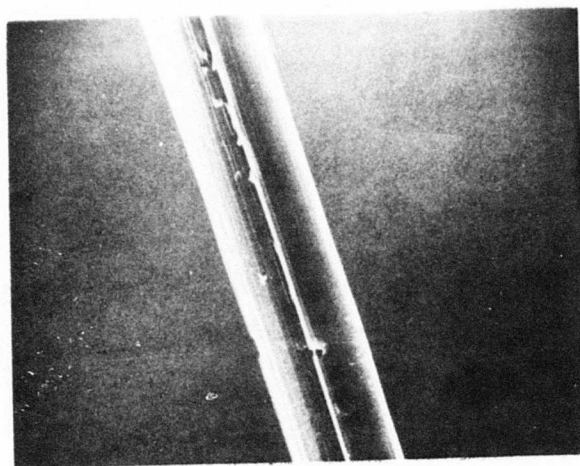
Figure 19 shows a typical scanning electron micrograph of a fiber from multifilament yarn which was thermoset by the two-stage method, heated to only 750°C, and air-etched at 520°C for 30 minutes. Most of the etching took place on the surface of the fiber, and many small pits were formed which had not been seen on fibers heated to 1650°C. The extensive surface etching of the fibers heated to 750°C is consistent with the high surface area at this processing stage, but the type of surface etching (formation of pits) was unexpected. The surface pits are probably a reflection of flaws in the fiber at this processing stage. These flaws, which are likely to be present in some form in the final carbonized fibers, are apparently revealed by etching at this processing stage. Another batch of the same pitch yarn was thermoset by the single stage method, and then processed and air etched in the identical manner. The yarn, in this case, was less severely etched; however, any filament which had been oxidized had an appearance similar to that shown in Figure 20, the pores being, perhaps, slightly smaller. The split in these radial fibers is still quite narrow at this stage. Figures 21 and 22 show several typical views of multifilament yarn fibers with radial structure, heat-treated at 1000°C, and air etched at 600°C for 30 minutes. Figure 21 reveals the radial structure in a particularly striking manner; in addition, the split in the fiber has opened to an angle of approximately 90°. The oxidation apparently takes place preferentially at the boundaries between the elongated domains which constitute the radial structure. Eventually, the fiber splits into ribbons visible in Figure 22. Obviously, the micro-fibrils in the fiber are subjected to considerable local stresses which, when released, cause the fibers to split and bend.

Etched fiber samples were also prepared from monofilaments with onion-skin or random structure, thermoset by either the single or two-stage methods and heat-treated to 750°C or 1000°C. The results were similar to those obtained for the multifilament yarn. The samples heat-treated to 750°C had small surface pits after etching, independent of the manner of thermosetting. Examples of this behavior are shown in the slightly etched filaments in Figure 23. Pores, such as that visible in the fracture surface in Figure 23a, were found in a number of the fibers in the batch of monofilament used for this experiment. After heat-treatment at 1000°C, the filaments also exhibited very similar behavior after etching. No surface pits were found, and almost all of the etching occurred at the boundaries of the elongated domains. However, Figure 24a shows what appears to be a slight skin-core effect in a lightly etched fiber prepared by the two-stage thermosetting method. This type of skin-core effect was not observed on lightly etched fibers thermoset by the single-stage method; this slight difference in the initial etching behavior is the only difference noted between the two 1000°C heat-treated samples. The skin in the sample prepared by the two-step method can be attributed to the first processing step which infusibilized the outer 1 - 2µm of the fiber. Figure 24b shows a fiber etched somewhat more than the previous one. The additional etching induced a more striated, but not pitted surface; the etching of the fiber end indicates that this fiber had an onion-skin structure.



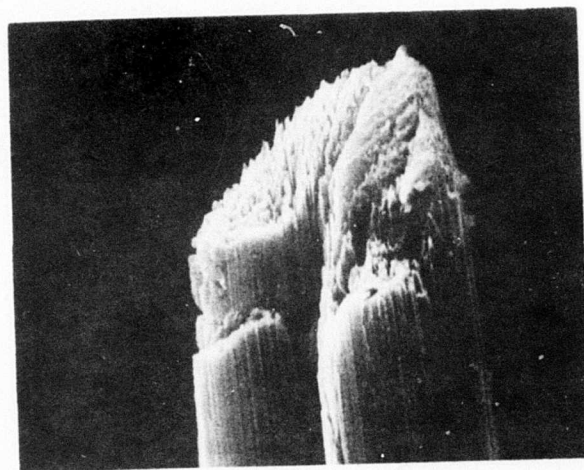
3000X

Figure 19. Scanning Electron Micrograph of a Fiber
Processed to 750°C, and Air-Etched at
520°C for 0.5 hour



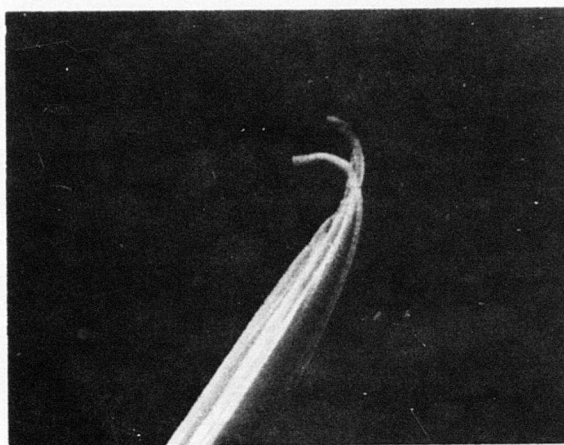
2000X

Figure 20. Scanning Electron Micrograph of a Fiber from Multifilament Yarn Thermoset by Single Stage Method, Heat-Treated to 750°C, and Air-Etched at 525°C for 0.5 hour



3000X

Figure 21. Scanning Electron Micrograph of a Fiber from Multifilament Yarn Thermoset by Single Stage Method, Heat-Treated to 1000°C, and Air-Etched at 600°C for 0.5 hour



2000X

a.



1000X

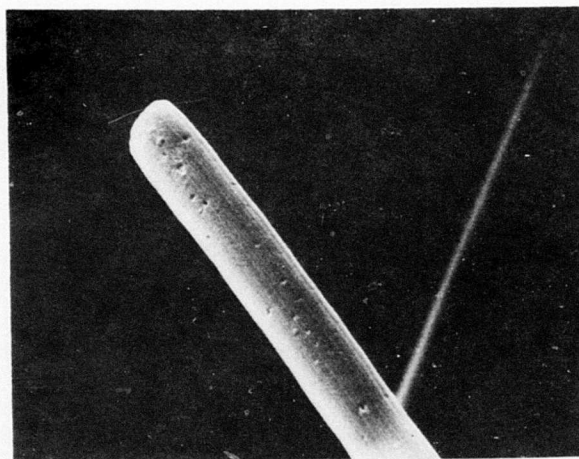
b.

Figure 22. Scanning Electron Micrographs of Fibers Processed to 1000°C, and Air-Etched at 600°C for 0.5 hour



3000X

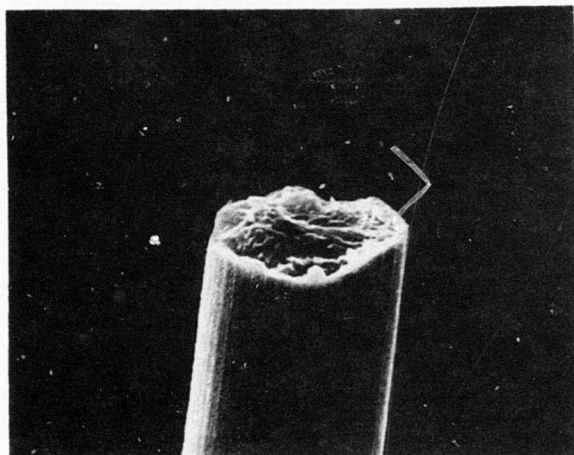
a.



2000X

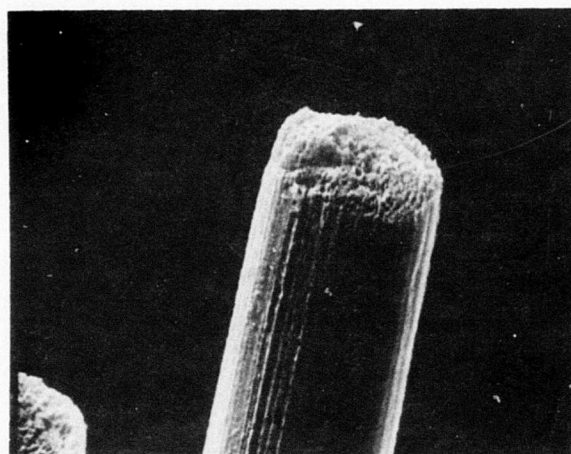
b.

Figure 23. Scanning Electron Micrographs of Monofilament Fibers, Thermoset by Single Stage Method, Heat-Treated to 750°C, and Air-Etched at 525°C for 0.5 hour



3000X

a.



3000X

b.

Figure 24. Scanning Electron Micrographs of Monofilament Fibers, Thermoset by the Two Stage Method, Heat-Treated to 1000°C, and Air-Etched at 550°C a, and 575°C b, for 0.5 hour

The results of this initial survey of etching behavior of pitch fibers at intermediate processing stages indicates that the dominant features in the etching behavior seem to be reflecting some local nonuniformities of the fiber at a given processing temperature rather than the effects resulting from the use of a particular thermosetting method.

5. Correlation of Fiber Structure with Single Filament Properties

In a paper presented at a recent American Ceramic Society Meeting, Davis and Sullivan⁽¹¹⁾ reported some single filament testing results on Type-P fibers. They obtained a sample of multifilament yarn which contained both round fibers having a nearly random structure and split or cracked fibers having a pronounced radial structure. They found that although the tensile strength of both types of fiber was comparable, the modulus of the split, radial fibers was significantly higher than that of the round fibers. Examination of our own testing results tended to support this result, but the data were not entirely convincing, mainly because the various multifilament yarn samples with different filament structures had not always been carbonized to the same final temperature.

Since the result reported by Davis and Sullivan was considered very significant, we decided to attempt to confirm their measurements. The procedure adopted consisted of obtaining long gauge (19.8 mm) single filament testing data for a number of filaments, preserving the portions of these individual filaments cemented to the mounting tabs used in testing and obtaining optical photomicrographs of the filament cross section of these portions of the filaments. The optical micrographs were used to measure the fiber cross-sectional area for comparison with the area calculated from the diameter determined by the split-image microscope technique used in fiber testing and also to determine whether a fiber was round or split. Suitable photomicrographs were obtained, and the average area determined from the photomicrographs for the ten filaments was within 10% of the average area determined by fiber testing. Next, forty filaments were tested from a sample known to contain about equal numbers of round and split filaments. Photomicrographs were obtained for the sections remaining on both ends of the tab for several filaments to determine some measure of the cross-sectional area variation along a ~3 cm length of the filament. Unexpectedly, a few of these filaments were found to be round at one of the tabs and split at the other end. In view of these findings, photomicrographs were obtained from both ends of the mounting tab for as many filaments as possible. Thirteen of the forty filaments were split in the original set of photomicrographs obtained for only one end of the tab. Photomicrographs of both ends of the tab could be obtained for only 25 filaments. Twenty of these filaments had the same structure (round or cracked) at both ends of the mounting tab, but five were split on one end and round at the other end of the mounting tab. The latter result indicates there could be a significant change in the fiber structure over a relatively short length of fiber. Efforts to confirm these findings by examining cross sections of long single filaments from the same sample at ~1 cm intervals are in progress.

The complication described above makes a correlation of fiber structure with modulus somewhat more tenuous. For that reason, only fibers with the same structure on both ends of the tab were used in comparison of the properties round and split filaments shown in Table VII. The average of the two areas determined for the ends of the filaments on the photomicrographs was used to recalculate the Young's modulus and tensile strength for each filament.

The fiber areas determined by the split-image microscope and the photomicrograph methods were nearly equal for the round fibers, but the fiber areas determined from the photomicrographs were considerably larger than those from the split-image microscope for the split filaments. Considerations discussed in Section IV 2. of this report apply here again.

The recalculated values for the properties of the round fibers are the same as those of the split fibers, within the rather large experimental errors. Although this result contrasts with that of Davis and Sullivan, the errors are so large in this study that it would be premature to draw conclusions, particularly when it appears that some of the fibers in the sample used here may have different structures at different points within the gauge length. Much more work of the type described above will be required to firmly establish the correlation of fiber properties with structure.

TABLE VII
FILAMENT PROPERTIES FOR ROUND AND SPLIT FIBERS
IN YARN SAMPLE LTF-17E

Fiber Type	Fiber Area (μm^2) FT ₍₁₎ OM ₍₂₎	Young's Modulus (GPa) FT ₍₁₎ OM ₍₂₎	Tensile Strength (GPa) FT ₍₁₎ OM ₍₂₎
Round (n = 15)	33.9 ± 6.7	272 ± 87	2.23 ± 0.27
Split (n = 5)	39.25 ± 2	363 ± 188	2.28 ± 0.32
			1.96 ± 0.23
			1.76 ± 0.17

(1) Averages and standard deviations for data and filament diameter from long gauge (19.8 mm) filament testing (F.T.).

(2) Averages and standard deviations using fiber areas measured on optical micrograph (O.M.) to re-evaluate fiber properties.

REFERENCES

- (1) Kimura and Habatu, U. S. Patent 3, 639, 953, Feb. 8, 1972.
- (2) Union Carbide Corporation, "Graphite Fibers from Pitch," Technical Report AFML-TR-73-147, Part II, March 1974, p.48.
- (3) A. Kelly, "Fiber Reinforcement of Metals," London, H.M.S.O. 1965.
- (4) D. Sinclair, J. Appl. Phys., 21, 380 (1950).
- (5) W. S. Williams, D. A. Steffens, and R. Bacon, J. Appl. Phys. 41, 4893 (1970).
- (6) S. Otani and S. Kimura, "Carbon Fibers," Tokyo, Japan, Kendai Henshusha Co. (1972).
- (7) Union Carbide Corporation, "Graphite Fibers from Pitch," Technical Report AFML-TR-73-147, Part II, March 1974, p. 58.
- (8) Union Carbide Corporation, "Graphite Fibers from Pitch," Technical Report AFML-TR-73-147, Part II, March 1974, p. 31.
- (9) R. Barnet and M. K. Noor, Carbon, 11, 281 (1973).
- (10) R. J. Diefendorf and E. W. Tokarsky, "The Relationships of Structure to Properties in Graphite Fibers," Technical Report AFML-TR-72-133, Part II, October 1973.
- (11) L. W. Davis & P. G. Sullivan, Amer. Ceramic Society Bull., 9/74, Abstract 2-CM-74P.

**THIS REPORT HAS BEEN DELIMITED
AND CLEARED FOR PUBLIC RELEASE
UNDER DOD DIRECTIVE 5200.20 AND
NO RESTRICTIONS ARE IMPOSED UPON
ITS USE AND DISCLOSURE.**

DISTRIBUTION STATEMENT A

**APPROVED FOR PUBLIC RELEASE,
DISTRIBUTION UNLIMITED.**